Iranian J Biotech. 2020 April;18(1): e2310 DOI: 10.30498/IJB.2020.137293.2310

Research Article

Enhancing Catecholase Activity of a Recombinant Human Tyrosinase Through Multiple Strategies

Arman Shahrisa[1], Maryam Nikkhah[2], Hadi Shirzad[3], Roudabeh Behzadi[4], Majid Sadeghizadeh[1]*

[1] Department of Genetics, Faculty of Biological Sciences, Tarbiat Modares University, Tehran, Iran
[2] Department of Nanobiotechnology, Faculty of Biological Sciences, Tarbiat Modares University, Tehran, Iran
[3] Department of Human Genetics, Faculty of Medical Sciences, Tarbiat Modares University, Tehran, Iran
[4] Department of Biology, Central Tehran Branch, Islamic Azad University, Tehran, Iran

**Corresponding author:* Majid Sadeghizadeh, Department of Genetics, Faculty of Biological Sciences, P.O. Box: 14115-154, Tarbiat Modares University, Tehran, Iran. Tel:+98-21-82884451, Fax: +98-21-82884717, E-mail: sadeghma@modares.ac.ir

Background: Tyrosinases are copper-containing enzymes that initiate the melanin synthesis. They catalyze the direct oxidation of L-tyrosine or L-DOPA into L-DOPAquinone.
Objectives: In present study, we aimed to obtain a recombinant tyrosinase with enhanced catecholase activity through site-directed mutagenesis.
Materials and Methods: The coding sequence of human tyrosinase along with native signal sequence was cloned into pET-28a (+). BL-21 was used as expression host and recombinant protein was purified by Ni-NTA resins. Site-directed mutagenesis was performed on M374 residue to achieve four mutants: M374D, M374T, M374K and M374R. Chloride ions (Cl^-) were removed from all solutions, and an extra amount of Cu^{2+} ions was added to recombinant tyrosinases by a novel technique during the purification process. Removal of Cl^- ions and addition of extra Cu^{2+} ions tripled catecholase activity of the recombinant protein. Therefore, all mutants were obtained under similar conditions.
Results: Although all the mutants presented higher catecholase activity in comparison to the wild-type enzyme, a significant increase in catecholase activity of the M374D mutant was observed – 13.2-fold. *In silico* modeling suggested that a *de novo* hydrogen bond occurs between side chain carboxyl oxygens of D374 and H367 in M374D. In the wild-type tyrosinase, the peptide oxygen atom of M374 is responsible for hydrogen bonding with H367.
Conclusions: Our data suggests that M374D mutational variant has applications in different areas such as agriculture, industry, and medicine.
Keywords: Catecholase activity; *E.coli*, Recombinant human tyrosinase; Site-directed mutagenesis

1. Background

Pigmentation of hair, skin, and eyes mainly depends on the quantity, quality, and distribution of melanin. In the sequential pathway of melanin formation, tyrosinase (EC 1.14.18.1) is the rate-limiting enzyme that initializes cascade reactions leading to the formation of melanin (1, 2). Tyrosinases are melanocytic copper containing enzymes (1, 3) that catalyze the direct oxidation of L-tyrosine (cresolase/monophenolase activity) or L-DOPA (catecholase/diphenolase activity) into L-DOPAquinone (2, 4). L-DOPAquinone is a highly reactive intermediate and therefore undergoes non-enzymatic and enzymatic reactions to form eumelanin and pheomelanin through separate pathways. Melanin synthesis is performed within specialized membrane-bound organelles known as melanosomes, and then those melanosomes are transferred to surrounding epidermal cells called keratinocytes (1, 5).

Tyrosinases along with catechol oxidases in plants and hemocyanins (oxygen carrier proteins) in arthropods comprise type-3 copper protein family. According to crystallographic evidence, all type-3 copper proteins share similar binuclear active site structure in which six conserved histidine residues coordinate a pair of copper atoms (CuA and CuB). During the catalytic reaction, type 3 copper centers exist in three forms. The deoxy form is inactive state of enzyme which binds molecular oxygen to provide the oxy form. The oxy form is capable of performing both cresolase and catecholase activities of tyrosinase while met form is only capable of performing cresolase activity (2, 6, 7). Despite the structural information provided by crystallographic results, the exact mechanism of catalytic reactions was unclear until recently (8).

Since tyrosinase is the initiating enzyme of melanogenesis pathway, any changes in coding region sequence, gene expression, protein folding, post-translational modifications or even in chemical environment of melanocytes can be associated with several disorders including malignant melanoma (9-11), oculocutaneous albinism 1 (OCA1) (12, 13) and vitiligo (14).

Production of human tyrosinase as a recombinant protein enables the researchers to further study the three-dimensional structure and catalytic mechanism of the enzyme and to find new tyrosinase inhibitors with fewer side effects. Moreover, the recombinant enzyme can be used in tyrosinase-based biosensors for measuring phenol content and other toxic compounds. Tyrosinases are helpful in detoxification of phenol-containing wastewater/soil, and synthesis of L-DOPA and Melanin. They are also useful in the production of cross-linked proteins (15), allowing biocatalysts such as lipase to be easily recycled.

2. Objectives

In the present study, we have produced recombinant human tyrosinase in *Escherichia coli*. This recombinant protein is produced in soluble form and can be readily purified by metal affinity chromatography. In addition, multiple strategies were considered to improve the catalytic activity of the recombinant protein including site-directed mutagenesis, addition of copper ions and removal of Cl ions.

3. Materials and Methods

3.1. Materials

T4 DNA ligase was purchased from Fermentas (Vilnius, Lithuania). Kanamycin, L-3,4-Dihydroxyphenylalanine (L-DOPA), and 30-kDa-cutoff dialysis membrane were obtained from Sigma-Aldrich (Shanghai, China). 3-Methyl-2-benzothiazolinon-hydrazon hydrochloride indicator (MBTH) was purchased from Merk *(*Darmstadt, Germany*)*. 1kb DNA ladder and protein marker (precision plus protein dual color standards) were obtained from SolisBioDyne (Tartu, Estonia) and Bio-Rad (Marne La Coquette, France) respectively.

3.2. Cloning the Tyrosinase Coding Sequence into pET-28a(+)

The complete coding sequence of human tyrosinase comprising native signal sequence was obtained from NCBI (NM_000372.4) and modified by the addition of *Eco*RI and *Hind*III restriction sites to 5′ and 3′ ends respectively (designated as hSTyr). hSTyr was synthesized in the pCR2.1 vector by EurofinsMWG/ Operon (Regensburg, Germany) The tyrosinase coding sequence was subcloned into the pET-28a(+) expression vector (Novagen, Madison, USA) between *Eco*RI and *Hind*III restriction sites. Chemically competent *E.coli* DH5α cells were transformed with the ligation products, and then the bacteria were cultured on the LB plate supplemented with50 $\mu g.mL^{-1}$ kanamycin. Recombinant colonies harboring pET-hSTyr (pET-28a(+) containing wild-type hSTyr) were identified by colony-PCR.

3.3. Site-Directed Mutagenesis

Site-directed mutagenesis was performed on pET-hSTyr according to QuikChange site-directed mutagenesis (Stratagene, La Jolla, USA) using four pairs of mutagenic primers. PCR conditions are as follows: one denaturation cycle at 94 ˚C for 1 min; 18 cycles of denaturation (94 ˚C, 30 sec), annealing (55 ˚C, 30 sec), and extension (68 ˚C, 14 min); plus a final extension cycle of 68 ˚C for 10 min. List of mutagenic primers has been shown in **Table 1**. PCR products were precipitated by ethanol and then treated by *Dpn*I (Fermentas, Vilnius, Lithuania) to eliminate template pET-hSTyr constructs. pET-hSTyr constructs with desired mutations M374D, M374K, M374T and M374R were respectively designated as pET-hSTyr(D), pET-hSTyr(K), pET-hSTyr(T) and pET-hSTyr(R).

Table 1. List of mutagenic primers was used for QuikChange site-directed mutagenesis. Substituted nucleotides are indicated in lower case.

Mutation	Forward primer	Reverse primer
M374D	5′-CTATATGAATGGAACAgatTCCCAGGTAC-3′	5′-GTACCTGGGAatcTGTTCCATTCATATAG-3′
M374T	5′-CTATATGAATGGAACAacaTCCCAGGTAC-3′	5′-GTACCTGGGAtgtTGTTCCATTCATATAG-3′
M374K	5′-CTATATGAATGGAACAaaaTCCCAGGTAC-3′	5′-GTACCTGGGAtttTGTTCCATTCATATAG-3′
M374R	5′-CTATATGAATGGAACAcgtTCCCAGGTAC-3′	5′-GTACCTGGGAgcaTGTTCCATTCATATA-3′

3.4. Protein Expression and Purification

Chemically competent *E.coli* BL21 cells were transformed with pET-hSTyr constructs (designated as BL21/pET-hSTyr) and the pre-culture was prepared by

introducing a colony into 5 mL modified LB broth (10 gr tryptone, 5 gr yeast extract, 2.31 gr KH_2PO_4, 12.54 gr K_2HPO_4 per liter) supplemented with 50 $\mu g.mL^{-1}$ kanamycin. After 16 hours, 4 mL of each pre-culture was added to 400 mL fresh TB broth (4 mL glycerol, 12 gr tryptone, 24 gr yeast extract, 2.31 gr KH_2PO_4, 12.54 gr K_2HPO_4 per liter) supplemented with 50 $\mu g.mL^{-1}$ kanamycin. Culture media were incubated at 37 ˚C while shaking until the OD_{600} reached to 0.6. Protein expression was induced by addition of 1 mM IPTG (Sigma-Aldrich, Germany) and then culture media was incubated at 18 ˚C for up to 16 hours with vigorous shaking. The cells were precipitated by spinning the cultures at 10,000 g for ten minutes at 4 °C.

Bacterial pellets were resuspended in equal volume of binding buffer and sonicated on ice for 15 cycles of 20-second pulses with 40-second intervals. The lysate was spun for 20 minutes at 12,000 g to separate soluble and insoluble fractions. Protein expression was assessed by SDS-PAGE analysis on a 10% polyacrylamide gel as described by Laemmli (16). BL21 cells harboring pET-28a(+) (designated as BL21/pET-28a(+)) were utilized as negative control for protein expression. After evaluation of protein quality by 10% SDS-PAGE, the supernatant was transferred to Ni-NTA columns.

Protein purification was performed under native conditions according to manufacturer's instruction. Each sample was loaded onto a 10 mL purification column containing 1 mL of Ni–NTA resins (Novagen, Darmstadt, Germany). Resins were first washed with 20 mL wash buffer (50 mM NaH_2PO_4, pH 8.0; 300 mM $(NH_4)_2SO_4$; 20 mM imidazole) supplemented with 100 µM $CuSO_4$ and subsequently by 20 mL wash buffer lacking $CuSO_4$ to remove free Cu^{2+} ions. Attached proteins were eluted by elution buffer (50 mM NaH_2PO_4, pH 8.0; 300 mM $(NH_4)_2SO_4$; 250 mM imidazole) and then dialyzed overnight against phosphate buffer (25 mM NaH_2PO_4-Na_2HPO_4, pH 6.8; 10% $v.v^{-1}$ of glycerol) at 4 ˚C. The protein concentration of each sample was determined by Bradford assay (17).

3.5. Measurement of the Catecholase Activity

The catecholase activity of each tyrosinase variant was measured according to a previously described method (18) with minor modifications. The reaction mixture (total volume 1.0 mL) was prepared by mixing 410 µL assay buffer (120 mM sodium phosphate pH 7.1, 5% $v.v^{-1}$ of *N,N'*-dimethyl formamide), 200 µL of 5 mM L-dopa, 290 µL of 20.7 mM MBTH to yield final concentrations of 50 mM sodium phosphate, 2% (by vol.) *N,N'*-dimethyl formamide, 1 mM L-dopa, 6 mM MBTH, and final pH of 6.9. The reaction mixture was incubated at 37 °C for 10 minutes. At the same time, purified tyrosinase was transferred from -20 ˚C to room temperature. Following the addition of tyrosinase to the reaction mixture and pipetting, the increase in absorbance at 505 nm was monitored (UV S-2100, Scinco, Korea) over a period of 10 minutes. The specific activity of each tyrosinase variant was expressed as means ± SD (standard deviation), and statistical differences were evaluated by ANOVA followed by Tukey's HSD (post-hoc test). $P<0.05$ was considered statistically significant.

3.6. In silico Analysis

In order to evaluate the effect of site-directed mutagenesis on the structure of recombinant human tyrosinase, required three-dimensional models were prepared by I-TASSER suite 4.1 (19). The full-length amino acid sequence of human tyrosinase along with attached N-terminal tags was given to I-TASSER suite. For each mutational variant, input sequence was altered to include the desired mutation. Obtained models were analyzed according to both C-score and evaluation results from SAVES (20-22) and PROSESS (23) metaservers. Superimposition and visualization of models were performed by UCSF Chimera v1.9 (24)

4. Results

4.1. Construction of pET-hSTyr, pET-hSTyr(D), pET-hSTyr(K), pET-hSTyr(T) and pET-hSTyr(R)

All pET-hSTyr (**Fig. 1**) vectors were verified by colony-PCR, double digestion by *Eco*RI and *Hind*III (**Fig.2**) and sequence analysis using universal and specific primers (**Supplementary data 1**). Sequencing results confirmed the presence of desired mutations without any additional mutation. **Figure 3** shows the structure of a transcript encoded by a pET-hSTyr construct.

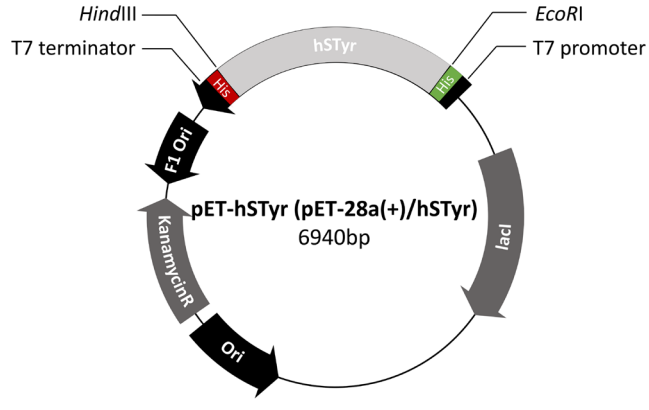

Figure 1. The Map of the pET-hSTyr expression vector.

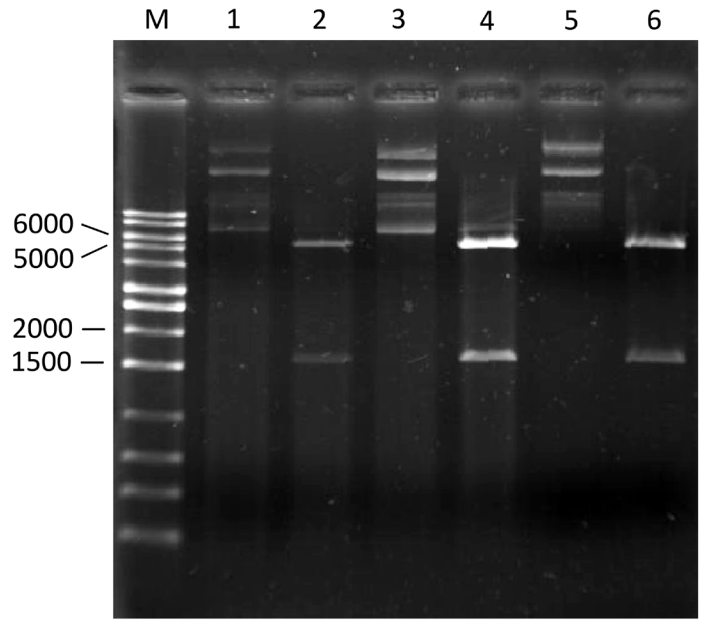

Figure 2. Double digestions of three pET-hSTyr constructs. M represents the DNA marker. 1 shows the intact pET-hSTyr construct while 2 shows the same construct after double digestion by *Eco*RI and *Hind*III. 3 and 4 represent intact construct and double digestion results for pET-hSTyr(D) respectively. 5 and 6 correspond to pET-hSTyr(T) construct and its double digestion result respectively.

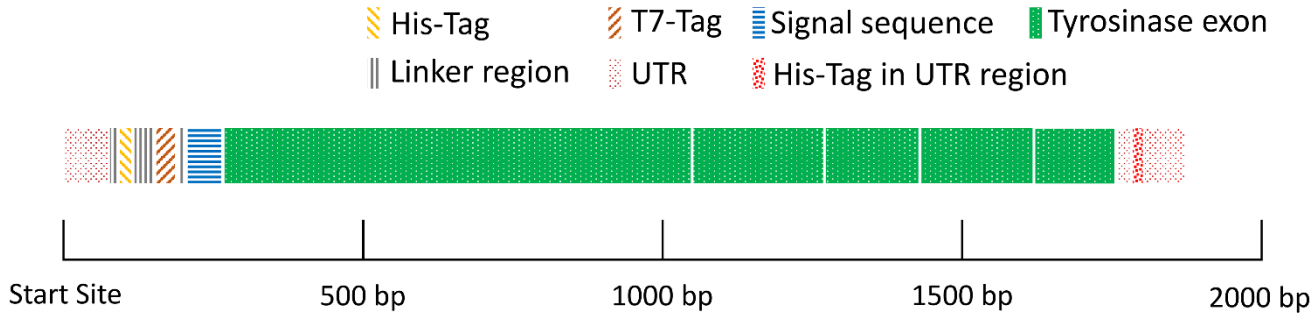

Figure 3. Schematic representation of full transcript which is coded by a pET-hSTyr construct. Each green segment represents a contiguous exon in a genomic region. 6x His-tag sequence adjacent to 3´ end is not translated due to the presence of native termination codon in tyrosinase sequence.

4.2. Protein Expression and Purification of Tyrosinases

Protein expression and purification were done as mentioned in material and methods. Purified enzymes were evaluated by 10% SDS-PAGE analysis, and then, the SDS-PAGE was assessed by TotalLab Quant software to determine the molecular weight of the purified tyrosinase. Unexpectedly, two adjacent bands with a molecular weight of 68 kDa and 65 kDa were visible on SDS-PAGE gel. (**Fig.4**). Since bacterial pellet was lysed in binding buffer supplemented with PMSF and all the procedures on the cell lysis were carried out using ice cold buffers, shorter isoform could be the result of the protease activity in the host cells.

4.3. Effect of Copper and Chloride Ions on the Catecholase Activity

Since, Cl^- ions are reversible tyrosinase inhibitors and can fully inactivate tyrosinase at a concentration of 800 mM (25-27), LB media was prepared with phosphate buffer instead of NaCl and TB media was chosen for protein expression since it lacks NaCl. Furthermore, Ni-NTA buffers were prepared with $(NH_4)_2SO_4$ rather than NaCl. On the other hand, it has long been known that presence of additional Cu^{2+} ions can enhance the activity of tyrosinases, but the reason is still unknown (28). In this study, Cu^{2+} ions were added to the recombinant proteins during the purification process, and the excess amount of copper ionswas removed by subsequent resin washes.

To examine the effect of additional Cu^{2+} ions on catecholase activity of the wild-type tyrosinase, half of the Ni-NTA resins with attached tyrosinase were transferred to another column. One column of resin-bound tyrosinases washed with normal washing buffer (designated as PSTyr), while the other column was first washed with the modified washing buffer supplemented with Cu^{2+} ions and then with normal washing buffer to remove free Cu^{2+} ions (designated as PSTyr-Cu^{2+}). Removal of free Cu^{2+} ions allows investigating the effect of attached Cu^{2+} ions. After protein purification and dialysis, PSTyr-Cu^{2+} exhibited a three-fold increase in the catecholase activity in comparison to PSTyr. Therefore, mutational variants were purified under similar conditions as described for PSTyr-Cu^{2+}.

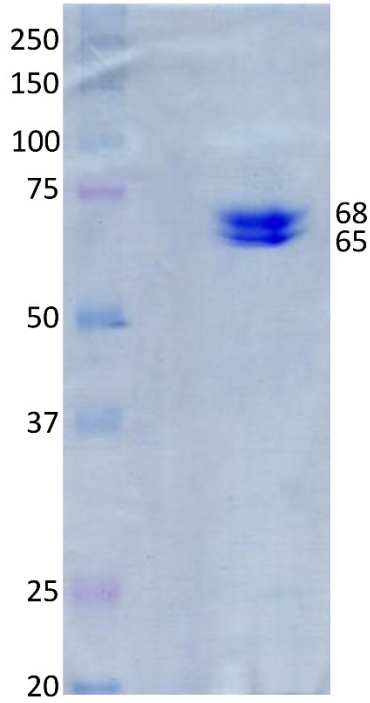

Figure 4. Purified wild-type tyrosinase. Purified tyrosinase consisted of two bands of 68 and 65 kDa. The former is the full-length enzyme, and the latter is formed probably due to slight proteolysis on the full-length isoform.

4.4. Effects of Site-Directed Mutagenesis on the Catecholase Activity

M374D mutational variant (designated as M374D-PSTyr-Cu^{2+}) exhibited a statistically significant 4.4-fold increase in the catecholase activity regarding PSTyr-Cu^{2+} (overall 13.2-fold increase regarding PSTyr). The differences in catecholase activity of the other mutational variants were not statistically significant. However, their catecholase activities were also higher than PSTyr-Cu^{2+}. M374T mutational variant (designated as M374T-PSTyr-Cu^{2+}) exhibited a two-fold increase in the catecholase activity as compared to PSTyr-Cu^{2+} (overall 6.1-fold increase comparing to PSTyr). The activities of two other mutational variants, M374K and M374R (respectively designated as M374K-PSTyr-Cu^{2+} and M374R-PSTyr-Cu^{2+}), were comparable with PSTyr-Cu^{2+}. The specific activities of all tyrosinase variants havebeen shown in **Table 2**.

Table 2. The measured specific activity of the different tyrosinase variants by MBTH assay. Catecholase activity of each variant was measured three times, and the mean value of measurements was used.

Sample	Specific activity (mmol min^{-1} mg^{-1}) ± S.E.
PSTyr	5.89 ± 0.5
PSTyr-Cu^{2+}	17.72 ± 0.3
PSTyr(M374D)-Cu2+	77.96 ± 3.2
PSTyr(M374T)-Cu2+	35.89 ± 0.3
PSTyr(M374K)-Cu2+	23.85 ± 0.5
PSTyr(M374R)-Cu^{2+}	18.74 ± 0.7

5. Discussion

In the present study, we achieved a tyrosinase mutant with significantly higher catecholase activity. This is the first study that uses site-directed mutagenesis in order to enhance catalytic activity of the human tyrossinase by targeting M374. In all type 3 copper proteins, two CuB alpha helixes are connected by a loop (connector loop). The loop also extends to the vicinity of the first CuA alpha helix and seems to be essential for the active site architecture (**Fig. 5a**). M374 and V377 are the most conserved residues in the loop. It has been suggested that the peptide bond oxygen atoms of these residues serve as hydrogen bond acceptors for the imidazole NH-groups of the two of the copper binding histidines. Therefore, these two hydrogen bonds stabilize active site architecture (29). The presence of V377 is limited to some tyrosinase species, and this residue does not exist in the other type-3 copper proteins. Moreover V205, which is the homologous residue of V377 in *Streptomyces castaneoglobisporus* tyrosinase, is not in the correct orientation to form a hydrogen bond with H38. Unexpectedly, two mutants created by substitution of V218 (homologous residue of V377) in *Bacillus megaterium* (V218G, and V218F) have exhibited higher catecholase activity in comparison to the wild-type enzyme (29). These observations have challenged the importance of V377 in the active site architecture. In contrast to V377, all resolved type 3 copper proteins possess a methionine residue at the same location as M374. This residue is densely packed

within the surrounding protein matrix, and its side chain extends into the space between two CuB alpha helixes (**Fig. 5a**). Interestingly, substitution of this methionine residue with a glycine has completely abolished the enzyme activity (30)

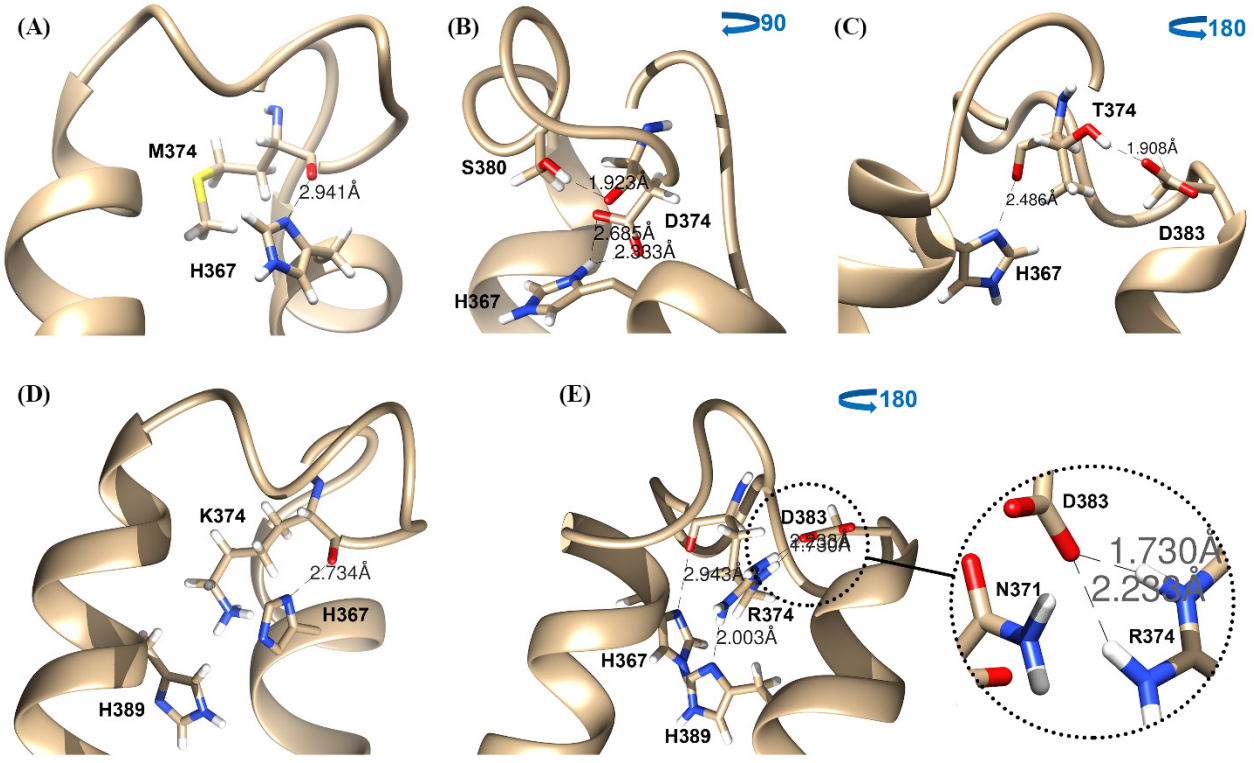

Figure 5. Predicted structure of different tyrosinase variants. All figures demonstrate two CuB alpha helixes along with the connector loop. **(A)** In PSTyr-Cu^{2+}, M374 forms a hydrogen bond with H367 through peptide bond oxygen. **(B)** In M374D-PSTyr-Cu^{2+}, both carboxyl oxygen atoms form a hydrogen bond with δ-nitrogen of H367. Unlike PSTyr-Cu^{2+}, peptide oxygen of D374 forms a hydrogen bond with the side chain of S380. **(C)** In M374T-PSTyr-Cu^{2+}, a hydrogen bond is formed between peptide bond oxygen of T374 and δ-nitrogen of H367. Another hydrogen bond is formed between T374 and D383. **(D)** In M374K-PSTyr-Cu^{2+}, peptide bond oxygen of K374 forms a hydrogen bond with δ-nitrogen of H367. Another hydrogen bond is also possible between side chain nitrogen of K374 and imidazole ring of H389. However, in our model imidazole ring of H389 is not in the correct orientation **(E)** In M374R-PSTyr-Cu^{2+}, peptide oxygen of R374 forms a hydrogen bond with δ-nitrogen of H367. Also, side chain guanidinium group of R374 forms two additional hydrogen bonds with δ-nitrogen of H389 and side chain carboxyl group of D383.

In the M374D-PSTyr-Cu^{2+}, both side chain carboxylate oxygen atoms of D374 are in the correct orientation regarding δ-nitrogen of H367 to form a hydrogen bond. In the wild-type tyrosinase, the peptide oxygen atom of M374 is responsible for hydrogen bonding with H367. This change in the pattern of hydrogen bonding can reorient the Cu_2O_2 complex which in turn increases the possibility of the catecholase reaction. Moreover, the distance between H367 and the connector loop is larger in comparison to that of the wild-type tyrosinase (**Fig. 5a, 5b**) which exposes the active site to the substrate. Further, peptide bond oxygen of D374 tends to form a hydrogen bond with S380, which results in conformational changes of connector loop.

In contrast to M374D-PSTyr-Cu^{2+}, mutated residues in the three other mutational variants form a hydrogen bond with H367 through their peptide oxygen atom similarly to wild-type tyrosinase (**Fig. 5c**, **5d**, and **5e**). In M374D-PSTyr-Cu^{2+}, there is another hydrogen bond between the side chain hydroxyl group of T374 and the side chain carboxyl group of D383 (**Fig. 5c**). Since D383 is on the connector loop, this substitution alters the conformation of two CuB alpha helixes. The resulting conformational change indirectly influences the orientation of Cu_2O_2 complex. Vital role of the connector loop in the orientation of Cu_2O_2 complex has been previously reported (29).

In M374K-PSTyr-Cu^{2+}, the second hydrogen bond is formed between the side chain of K374 and H389 (**Fig. 5d**), which is an essential residue for the correct orientation of the substrate toward Cu_2O_2 complex (31). In this mutant, the imidazole ring of H389 is not

in the right orientation to form the mentioned hydrogen bond in our model. As the Lysine possesses larger side chain in comparison to methionine, it enters the space between two CuB alpha helices. This can cause a conformational change and influence the orientation of Cu_2O_2 complex.

M374R-PSTyr-Cu^{2+} exhibited very close results to PSTyr-Cu^{2+} (**Fig. 5e**). In addition to the mentioned hydrogen bonding between peptide oxygen of R374 and H367, there are at least two other hydrogen bonds: guanidinium group of R374 and δ-nitrogen of H389, and guanidinium group of R374 and the side chain carboxyl group of D383. The side chain of R374 seems to be involved in the formation of the largest number of hydrogen bonds among all the mutational variants. Despite this prediction, specific activity measurements showed that there is not a significant difference in catecholase activity between M374R-PSTyr-Cu^{2+} and PSTyr-Cu^{2+}.

In the previous studies (32, 33), cloning the coding sequence of human tyrosinase resulted in the formation of mainly inclusion bodies. On the contrary, our recombinant enzyme was obtained in soluble form. In addition, wild-type recombinant protein which is produced in our research possesses remarkable catecholase activity compared to the previous studies where only the small soluble fraction exhibited remarkable catecholase activity. Further, this is the first report of mutagenesis of M374 which resulted in tyrosinase variant with higher catecholase activity. Recently, another research has obtained recombinant human tyrosinase from insect cells (34). Unfortunately, as the activity is not reported as specific activity, it is not comparable to our work.

5.1. Effects of Glycosylation and Phosphorylation

M374 is located after a conserved ^{371}NGT^{373} glycosylation sequon (35, 36). It has been reported that presence of N-glycans at N337 and N371 is required for proper folding of tyrosinaseand the absence of N-glycans at N86, N111 and N161 resulted in temperature-sensitive mutants (37). Another report states that the absence of N-glycosylation at N86, N230, N337 and N371 abolishes tyrosinase activity (38). Similarly, inhibition of glycosylation by tunicamycin exerts a similar effect (39, 40). More interestingly, N371K is one of the mutations causing oculocutaneous albinism IA (41). On the other hand, it has been demonstrated that PKC-β is involved in phosphorylation of melanosomal tyrosinase and this enhances protein activity (42, 43). It is important to note that all natural modifications occurring on nascent human tyrosinase, ultimately influence the orientation of Cu_2O_2 complex. That's why two studies (32, 33) conducted previously in parallel with our study have successfully produced the active protein in *E. coli*. At a glance, these reports look confusing, but it is possible to offer multiple explanations for these controversial observations. As it is more difficult to extract considerable amount of any desired protein from eukaryotes, activity measurements in the previous studies have been reported as relative activities rather than specific activities. We suggest that the specific activity of the wild-type tyrosinase which is obtained from eukaryotic hosts should be much higher than the recombinant protein that is obtained from *E. coli* cells due to the presence of the perfect post-translational modifications in eukaryotic cells. However, higher amount of the recombinant enzymes obtained from *E. coli* enables measuring the catecholase activity. In addition, glycans act as quality labels during the maturation of the proteins in eukaryotic cells. It can be suggested that the lack of glycosylation at N371 in tyrosinase leads to ER retention and degradation of tyrosinase by cell proteasome (44) and subsequently the loss of tyrosinase activity. Finally, as glycosylation can influence the orientation of Cu_2O_2 complex, mutations with higher catalitic activity must have possessed better oriented Cu_2O_2 complex.

6. Conclusion

The present research has focused on the production of soluble recombinant tyrosinase in *E. coli*. Two unique strategies were considered, removal of Cl^- ions and addition of copper ions, to enhance the activity of obtained recombinant wild-type tyrosinase. The addition of copper ions to the wash buffer effectively increased catecholase activity without leaving any adverse effect on Ni-NTA resins. Furthermore, site-directed mutagenesis was applied to achieve mutants with enhanced catecholase activity. Although all mutants possessed higher activity in comparison to the wild-type enzyme, one of the mutants exhibited a substantial increase in the catecholase activity. Obtained tyrosinases are suitable for application in different fields such as agriculture, industry, and medicine.

Funding

This study was supported by two independent grants from Iran National Science Foundation (INSF) and Tarbiat Modares University.

Conflicts of Interest

Authors declare competing for financial interest about all the achievements of the present study.

Ethical Approval

This article does not contain any studies with human participants or animals performed by any of the authors.

Acknowledgment

Authors acknowledge Dr. Reza H Sajedi for providing Ultrafiltration Disc and his helpful advice. Authors also wish to thank Prof. Aziz Shahrisa, Dr. Seyed Shahriar Arab, Shirin Shahangian, Soheila Mohammadi, Milad Balazadeh and Marzieh Karimi for their valuable guidance as well as Pedram Chavoshipour Heris for his help in proofreading the manuscript. This work was supported by TMU and INSF (Iran National Science Foundation) financial aids.

References

1. Bae-Harboe YS, Park HY. Tyrosinase: a central regulatory protein for cutaneous pigmentation. *J Invest Dermatol*. 2012;**132**(12):2678-2680. doi:10.1038/jid.2012.324
2. Ramsden CA, Riley PA. Tyrosinase: the four oxidation states of the active site and their relevance to enzymatic activation, oxidation and inactivation. *Bioorg Med Chem*. 2014;**22**(8):2388-2395. doi:10.1016/j.bmc.2014.02.048
3. Wang N, Daniels R, Hebert DN. The cotranslational maturation of the type I membrane glycoprotein tyrosinase: the heat shock protein 70 system hands off to the lectin-based chaperone system. *Mol Biol Cell*. 2005;**16**(8):3740-3752. doi:10.1091/mbc.E05-05-0381
4. Cooksey CJ, Garratt PJ, Land EJ, Pavel S, Ramsden CA, Riley PA, *et al*. Evidence of the indirect formation of the catecholic intermediate substrate responsible for the autoactivation kinetics of tyrosinase. *J Biol Chem*. 1997;**272**(42):26226-26235. doi:10.1074/jbc.272.42.26226
5. Ito S, Wakamatsu K. Chemistry of Mixed Melanogenesis—Pivotal Roles of Dopaquinone. *Photochem Photobiol*. 2008;**84**(3):582-592. doi:10.1111/j.1751-1097.2007.00238.x
6. Matoba Y, Kumagai T, Yamamoto A, Yoshitsu H, Sugiyama M. Crystallographic evidence that the dinuclear copper center of tyrosinase is flexible during catalysis. *J Biol Chem*. 2006;**281**(13):8981-8990. doi:10.1074/jbc.M509785200
7. Aguilera F, McDougall C, Degnan BM. Origin, evolution and classification of type-3 copper proteins: lineage-specific gene expansions and losses across the Metazoa. *BMC Evol Biol*. 2013;**13**:96. doi:10.1186/1471-2148-13-96
8. Goldfeder M, Kanteev M, Isaschar-Ovdat S, Adir N, Fishman A. Determination of tyrosinase substrate-binding modes reveals mechanistic differences between type-3 copper proteins. *Nat Commun*. 2014;**5**:4505. doi:10.1038/ncomms5505
9. Gudbjartsson DF, Sulem P, Stacey SN, Goldstein AM, Rafnar T, Sigurgeirsson B, *et al*. ASIP and TYR pigmentation variants associate with cutaneous melanoma and basal cell carcinoma. *Nat Genet*. 2008;**40**(7):886-891. doi:10.1038/ng.161
10. Bishop DT, Demenais F, Iles MM, Harland M, Taylor JC, Corda E, *et al*. Genome-wide association study identifies three loci associated with melanoma risk. *Nat Genet*. 2009;**41**(8):920-925. doi:10.1038/ng.411
11. Pervolaraki E, Lobach I, Belitskaya-Levy I, Ostrer H, Goldberg J, Polsky D, *et al.*, editors. Identification of tyrosinase polymorphisms for use in melanoma risk assessment. *J Clin Oncol* (Meeting Abstracts); 2010.
12. Oetting WS. The tyrosinase gene and oculocutaneous albinism type 1 (OCA1): A model for understanding the molecular biology of melanin formation. *Pigment Cell Res*. 2000;**13**(5):320-325. doi:10.1034/j.1600-0749.2000.130503.x
13. Kamaraj B, Purohit R. Mutational analysis of oculocutaneous albinism: a compact review. *Biomed Res Int.* 2014;**2014**:10. doi:10.1155/2014/905472
14. Yaghoobi R, Omidian M, Bagherani N. Vitiligo: A review of the published work. *J Dermatol.* 2011;**38**(5):419-431. doi:10.1111/j.1346-8138.2010.01139.x
15. Zaidi KU, Ali AS, Ali SA, Naaz I. Microbial tyrosinases: promising enzymes for pharmaceutical, food bioprocessing, and environmental industry. *Biochem Res Int.* 2014;**2014**:854687. doi:10.1155/2014/854687
16. Laemmli UK. Cleavage of structural proteins during the assembly of the head of bacteriophage T4. *Nature*. 1970;**227**(5259):680-685.
17. Bradford MM. A rapid and sensitive method for the quantitation of microgram quantities of protein utilizing the principle of protein-dye binding. *Anal Biochem*. 1976;**72**(1-2):248-254. doi:10.1016/0003-2697(76)90527-3
18. Winder AJ, Harris H. New assays for the tyrosine hydroxylase and dopa oxidase activities of tyrosinase. Eur J Biochem. 1991;**198**(2):317-26.
19. Yang J, Yan R, Roy A, Xu D, Poisson J, Zhang Y. The I-TASSER Suite: protein structure and function prediction. *Nat Methods*. 2014;**12**(1):7-8. doi:10.1038/nmeth.3213
20. Laskowski RA, MacArthur MW, Moss DS, Thornton JM. PROCHECK: a program to check the stereochemical quality of protein structures. *J Appl Crystallogr*. 1993;**26**(2):283-291. doi:10.1107/s0021889892009944
21. Colovos C, Yeates TO. Verification of protein structures: patterns of nonbonded atomic interactions. *Protein Sci.* 1993;**2**(9):1511-1519. doi:10.1002/pro.5560020916
22. Eisenberg D, Lüthy R, Bowie JU. VERIFY3D: Assessment of protein models with three-dimensional profiles. *Methods Enzymol.* 1997;**277**:396-404. doi:10.1016/s0076-6879(97)77022-8
23. Berjanskii M, Liang Y, Zhou J, Tang P, Stothard P, Zhou Y, et al. PROSESS: a protein structure evaluation suite and server. *Nucleic Acids Res*. 2010;**38**(Web Server issue):W633-W40. doi:10.1093/nar/gkq375
24. Pettersen EF, Goddard TD, Huang CC, Couch GS, Greenblatt DM, Meng EC, *et al.* UCSF Chimera--a visualization system for exploratory research and analysis. *J Comput Chem*. 2004;**25**(13):1605-1612. doi:10.1002/jcc.20084
25. Lerner AB. Mammalian tyrosinase: Effect of ions on enzyme action. *Arch Biochem Biophys*. 1952;**36**(2):473-481. doi:10.1016/0003-9861(52)90435-9
26. Park YD, Kim SY, Lyou YJ, Lee JY, Yang JM. A new type of uncompetitive inhibition of tyrosinase induced by Cl-binding. *Biochimi*e. 2005;**87**(11):931-937. doi:10.1016/j.biochi.2005.06.006
27. Han HY, Lee JR, Xu WA, Hahn MJ, Yang JM, Park YD. Effect of Cl- on tyrosinase: complex inhibition kinetics and biochemical implication. *J Biomol Struct Dyn*. 2007;**25**(2):165-171. doi:10.1080/07391102.2007.10507165
28. Kupper U, Linden M, Cao K, Lerch K. Expression of tyrosinase in vegetative cultures of Neurospora crassa transformed with

a metallothionein promoter/protyrosinase fusion gene. *Current Genetics*. 1990;**18**(4)31331-5. doi:10.1007/bf00318214
29. Goldfeder M, Kanteev M, Adir N, Fishman A. Influencing the monophenolase/diphenolase activity ratio in tyrosinase. *Biochim Biophys Acta.* 2013;**1834**(3):629-633. doi:10.1016/j.bbapap.2012.12.021
30. Schweikardt T, Olivares C, Solano F, Jaenicke E, Garcia-Borron JC, Decker H. A three-dimensional model of mammalian tyrosinase active site accounting for loss of function mutations. *Pigment Cell Res*. 2007;**20**(5):394-401. doi:10.1111/j.1600-0749.2007.00405.x
31. Olivares C, García-Borrón JC, Solano F. Identification of Active Site Residues Involved in Metal Cofactor Binding and Stereospecific Substrate Recognition in Mammalian Tyrosinase. Implications to the Catalytic Cycle†. *Biochemistry*. 2002;**41**(2):679-686. doi:10.1021/bi011535n
32. Kong K-H, Park S-Y, Hong M-P, Cho S-H. Expression and characterization of human tyrosinase from a bacterial expression system. *Comp Biochem Physiol B Biochem Mol Biol*. 2000;**125**(4):563-569. doi:10.1016/s0305-0491(00)00163-2
33. Chen GH, Chen WM, Huang YC, Jiang ST. Expression of recombinant mature human tyrosinase from Escherichia coli and exhibition of its activity without phosphorylation or glycosylation. *J Agric Food Chem.* 2012;**60**(11):2838-2843. doi:10.1021/jf205021g
34. Lai X, Soler-Lopez M, Wichers HJ, Dijkstra BW. Large-Scale Recombinant Expression and Purification of Human Tyrosinase Suitable for Structural Studies. *PLoS One*. 2016;**11**(8):e0161697. doi:10.1371/journal.pone.0161697
35. Garcia-Borron JC, Solano F. Molecular Anatomy of Tyrosinase and its Related Proteins: Beyond the Histidine-Bound Metal Catalytic Center. *Pigment Cell Research*. 2002;**15**(3):162-173. doi:10.1034/j.1600-0749.2002.02012.x
36. Olivares C, Solano F, Garcia-Borron JC. Conformation-dependent post-translational glycosylation of tyrosinase. Requirement of a specific interaction involving the CuB metal binding site. *J Biol Chem*. 2003;**278**(18):15735-15743. doi:10.1074/jbc.M300658200
37. Halaban R, Cheng E, Hebert DN. Coexpression of wild-type tyrosinase enhances maturation of temperature-sensitive tyrosinase mutants. *J Invest Dermatol*. 2002;**119**(2):481-478. doi:10.1046/j.1523-1747.2002.01824.x
38. Branza-Nichita N, Negroiu G, Petrescu AJ, Garman EF, Platt FM, Wormald MR, et al. Mutations at Critical N-Glycosylation Sites Reduce Tyrosinase Activity by Altering Folding and Quality Control. *J Biol Chem*. 2000;**275**(11):8169-8175. doi:10.1074/jbc.275.11.8169
39. Imokawa G, Mishima Y. Biochemical characterization of tyrosinase inhibitors using tyrosinase binding affinity chromatography. *Br J Dermatol*. 1981;**104**(5):531-539. doi:10.1111/j.1365-2133.1981.tb08167.x
40. Takahashi H, Parsons PG. Rapid and Reversible Inhibition of Tyrosinase Activity by Glucosidase Inhibitors in Human Melanoma Cells. *J Invest Dermatol*. 1992;**98**(4):481-487. doi:10.1111/1523-1747.ep12499862
41. Gershoni-Baruch R, Rosenmann A, Droetto S, Holmes S, Tripathi RK, Spritz RA. Mutations of the tyrosinase gene in patients with oculocutaneous albinism from various ethnic groups in Israel. *Am J Hum Genet*. 1994;**54**(4):586.
42. Park H-Y, Russakovsky V, Ohno S, Gilchrest B. The beta isoform of protein kinase C stimulates human melanogenesis by activating tyrosinase in pigment cells. *J Biol Chem*. 1993;**268**(16):11742-11749.
43. Park H-Y, Perez JM, Laursen R, Hara M, Gilchrest BA. Protein kinase C-β activates tyrosinase by phosphorylating serine residues in its cytoplasmic domain. *J Biol Chem*. 1999;**274**(23):16470-16478.
44. Halaban R, Svedine S, Cheng E, Smicun Y, Aron R, Hebert DN. Endoplasmic reticulum retention is a common defect associated with tyrosinase-negative albinism. *Proc Natl Acad Sci USA*. 2000;**97**(11):5889-5894. doi:10.1073/pnas.97.11.5889